Modern Pathology (2014) 27, 1394–1404

Visual and automated assessment of matrix metalloproteinase-14 tissue expression for the evaluation of ovarian cancer prognosis

Dominique Trudel[1,2,5], Patrice Desmeules[3,5], Stéphane Turcotte[1], Marie Plante[1,4], Jean Grégoire[4], Marie-Claude Renaud[4], Michèle Orain[3], Isabelle Bairati[1] and Bernard Têtu[1,3]

[1]Laval University Cancer Research Center and Research Center of the Centre Hospitalier Universitaire (CHU) de Québec, Québec, Canada; [2]Department of Pathology/Applied Molecular Oncology, Toronto General Hospital, University Health Network, Toronto, Ontario, Canada; [3]Anatomic Pathology and Cytology Department, Hôpital du St-Sacrement, Centre Hospitalier Universitaire (CHU) de Québec, Laval University, Québec, Canada and [4]Gynecologic Oncology Division, Centre Hospitalier Universitaire (CHU) de Québec, Québec, Canada

The purpose of this study was to evaluate whether the membrane type 1 matrix metalloproteinase-14 (or MT1-MMP) tissue expression, as assessed visually on digital slides and by digital image analysis, could predict outcomes in women with ovarian carcinoma. Tissue microarrays from a cohort of 211 ovarian carcinoma women who underwent a debulking surgery between 1993 and 2006 at the *CHU de Québec* (Canada) were immunostained for matrix metalloproteinase-14. The percentage of MMP-14 staining was assessed visually and with the Calopix software. Progression was evaluated using the CA-125 and/or the RECIST criteria according to the GCIG criteria. Dates of death were obtained by record linkage with the Québec mortality files. Adjusted hazard ratios of death and progression with their 95% confidence intervals were estimated using the Cox model. Comparisons between the two modalities of MMP-14 assessment were done using the box plots and the Kruskal–Wallis test. The highest levels of MMP-14 immunostaining were associated with nonserous histology, early FIGO stage, and low preoperative CA-125 levels ($P<0.05$). In bivariate analyses, the higher level of MMP-14 expression (>40% of MMP-14-positive cells) was inversely associated with progression using visual assessment (hazard ratio = 0.39; 95% confidence interval: 0.18–0.82). A similar association was observed with the highest quartile of MMP-14-positive area assessed by digital image analysis (hazard ratio = 0.48; 95% confidence interval: 0.28–0.82). After adjustment for standard prognostic factors, these associations were no longer significant in the ovarian carcinoma cohort. However, in women with serous carcinoma, the highest quartile of MMP-14-positive area was associated with progression (adjusted hazard ratio = 0.48; 95% confidence interval: 0.24–0.99). There was no association with overall survival. The digital image analysis of MMP-14-positive area matched the visual assessment using three categories (>40% *vs* 21–40 *vs* <20%). Higher levels of MMP-14 immunostaining were associated with standard factors of better ovarian carcinoma prognosis. In women with serous carcinoma, high expression of MMP-14 was associated with lower progression.

Modern Pathology (2014) **27,** 1394–1404; doi:10.1038/modpathol.2014.32; published online 7 March 2014

Keywords: digital image analysis; immunohistochemistry; matrix metalloproteinase-14; ovarian carcinoma; prognosis

In the western world, ovarian cancer is the leading cause of death among gynecological malignancies and the fifth leading cause of cancer death.[1–3] Most patients present with advanced stage disease, partly because of its anatomic location, nonspecific symptoms, and lack of reliable screening methods. Despite a high rate of complete remission rate after radical surgery followed by taxane and platinum-based chemotherapy, relapse occurs in the majority

Correspondence: Dr D Trudel, MD, PhD, Laval University Cancer Research Center and Research Center of the Centre Hospitalier Universitaire (CHU) de Québec, 11 Côte du Palais, Québec, Québec G1R 2J6, Canada.
E-mail: Dominique.Trudel.3@ulaval.ca
[5]The first two authors contributed equally to this work.
Received 20 September 2013; revised 18 December 2013; accepted 19 December 2013; published online 7 March 2014

of patients with advanced disease.[4] Long-term survival of such patients is as low as 10 to 30%.[5,6] Up to now, exploration of potent chemoresistance markers on ovarian carcinoma identified only a few factors being linked to progression-free survival.

Growing evidence supports a role for extracellular proteinases to mediate changes in the microenvironment during tumor progression and therefore modify tumoral behavior. Among them figure the matrix metalloproteinases (MMPs), a family of over 20 zinc-dependent endopeptidases either secreted or bounded to plasma membranes.[7] These proteins are thought to play a direct role in cell adhesion and migration, cell contact disruption, tumor angiogenesis, and proteolytic processing of cytokine and growth factors, thus playing a key role in the complex tumorigenesis process. The function of MMPs is partly regulated by four known endogenous inhibitors (tissue inhibitor of metalloproteinases (TIMPs) 1 to 4) that are also expressed at tumor sites.[8–10]

The metalloproteinase 14 (or membrane-type 1 matrix metalloproteinase (MT1-MMP)) is a membrane-anchored collagenase that degrades collagen type I to III and other extracellular matrix proteins. At the cell surface, MMP-14 binds to tissue inhibitor of metalloprotease-2 and the secreted pro-MMP-2, forming a trimolecular complex that results in the activation and release of active MMP-2 (Gelatinase A).[11,12] The presence of MMP-14 in ovarian tumor and stromal cells has been demonstrated[13–15] and related with worse prognosis in a study including 90 women with ovarian cancer.[16] The presence of high levels of mRNA in metastatic implants was also associated with a worse prognostic, but not independently.[17] More studies are needed before the clinical implementation of MMP-14 can be used as a tumor marker to predict ovarian cancer prognosis.

Furthermore, a reliable evaluation method needs to be established in order to instigate the use of a new clinical biomarker. Unfortunately, intra- and inter-observer variability limits the reliability of immunohistochemical biomarker quantification. Digital image analysis is a potential approach to obtain faster and more objective measures than using conventional microscopy. Although the combined evidence suggests that digital image analysis is able to reproduce manual data at an acceptable level, it must be compared with the gold standard that is the semiquantitative visual estimation done by pathologists.[18,19]

The purpose of this study was to evaluate whether the tissue expression of MMP-14, as assessed by a semiquantitative method by pathologists and by an automated digital image analysis, could predict the occurrence of progression and death in women with ovarian carcinoma. In order to accelerate clinical implementation, we also developed a digital image analysis method and validated its use by comparing it with visual immunostaining quantification.

Materials and methods

Patients and Data Collection

Patients included in this study were women who underwent cytoreductive surgery for ovarian carcinoma between 1993 and 2006 at l'Hôtel-Dieu de Québec of the Centre Hospitalier Universitaire de Québec (CHU de Québec), Canada. Women were included if they had an ovarian carcinoma of any FIGO stage treated with debulking surgery and adjuvant chemotherapy when indicated.[20] Those who received neoadjuvant chemotherapy were excluded. All women provided a written consent to participate with the tumor bank as approved by the local Research Ethics Board.

The CHU de Québec medical files were reviewed to collect age, clinicopathological characteristics (FIGO stage, histology, grade, preoperative CA-125), and treatment modalities at the time of the cytoreductive surgery (residual tumor, modalities of chemotherapy). Progression after first-line therapy was defined according to CA-125 levels and/or the Response Evaluation Criteria in Solid Tumours (RECIST) criteria[21] as proposed by the Gynecologic Cancer InterGroup (GCIG).[22] When progression was documented using both criteria, we recorded the date of the earliest event as the date of progression. Clinical follow-up was obtained from the medical files and was updated regularly until June 2012. Date and cause of death were obtained by record linkage with the Québec mortality files using the Québec health insurance unique identifier.

Tissue Microarray Construction

The diagnostic slides were reviewed by two pathologists (BT and DT) to confirm histological subtype and grade[23] and to select the most representative paraffin block from each tumor. Three representative 0.6 mm tumor cores were embedded on a recipient paraffin block with a tissue arrayer (Beecher Instruments Tissue Microarray Technology, Estigen, Sun Prairie, WI, USA). The triplicates were randomly distributed on one of five recipient blocks in order to avoid immunohistochemistry evaluation bias.

Immunohistochemistry

From tissue array blocks, 4-μm-thick sections were cut. Sections were deparaffinized in toluene and rehydrated in graded alcohols, then incubated with 3% hydrogen peroxide for 10 min, followed by blocking serum for 20 min. Sections were then incubated with a rabbit polyclonal anti-MMP-14 polyclonal antibody (cat. no. PA1-38193, Pierce, Thermo Scientific, IL, USA) at room temperature for 1 h in a 1 : 1000 dilution in phosphate-buffered saline (PBS), pH 7.4, with 1% bovine serum albumin. Detection was completed following the avidin-biotin method using the Super Stain HRP kit

(cat. no. IDMR-2001, IDLabs, London, ON, Canada), revealed by 3,3′-diaminobenzidine (DAB; cat. no. BP1110, IDLabs) and counterstained with Harris hematoxylin. Sections from prostate carcinoma with known positivity were used as positive controls. Antibody diluent was used instead of primary antibody on negative controls.

Slide Digitization and Pathologist Visual Scoring

Digital images of immunohistochemically stained tissue microarray slides were obtained at $\times 20$ magnification using a slide scanner (NanoZoomer 2.0-HT, Hamamatsu, Bridgewater, NJ, USA). Images were loaded and visualized using a specialized server (mScope, Aurora Interactive, Montréal, Canada).

Each tissue microarray spot with $>30\%$ of its surface covered by tumor was evaluated independently for MMP-14 immunostaining by two observers (PD and DT), without knowledge of clinical data. The percentage of tumor cells expressing the marker was assessed using an interval scale (0%, 1–20%, 21–40%, 41–60%, 61–80%, and 81–100%). The intensity of staining was evaluated using four levels of intensity (absence (0), low (1), moderate (2), high (3)). For each of these variables, when a difference of two or more levels was noted between the first two reviews, a third senior pathologist (BT) reviewed the case. Discrepancies between results with a difference of one level were reviewed by the two first pathologists to reach a consensus. Cases with two or more interpretable tissue microarray spots were retained for the statistical analyses.

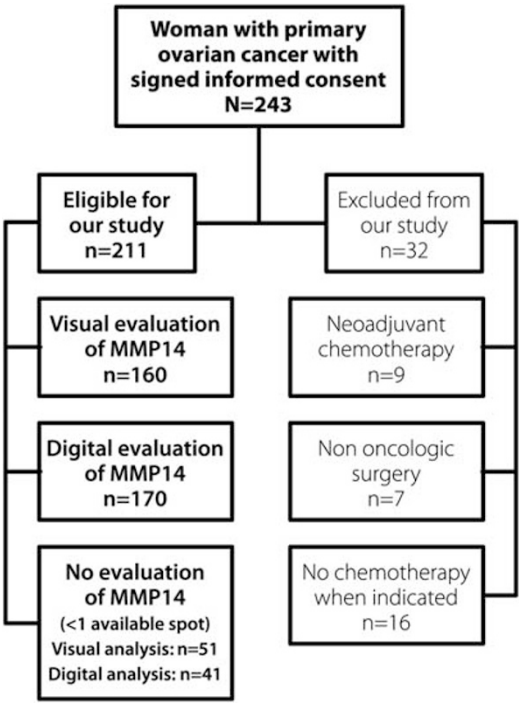

Figure 1 Study flowchart.

Digital Image Analysis

Automated immunohistochemistry measurements were performed using Calopix software (developed by TRIBVN (Châtillon, France), distributed by Agfa Healthcare (Toronto, ON, Canada)). The Ilastik 5.0 Interactive Learning and Segmentation Toolkit that allows for tissue recognition was used within Calopix in order to analyze only the epithelial component. The Calopix 'immunosurface' software was then applied to each spot. To develop the immunosurface algorithm, four intensity classes (0, 1, 2, and 3) were first defined in the epithelial component. A mean nuclear surface ($5 \times 5\,\mu$m) was then attributed and used in the algorithm to estimate the number of cells within the tissue surface detected. The algorithm then generated an output including the total area of epithelial tissue detected, the ratio (as percentage and cell number) of positive tissue area, and the ratio (as percentage and cell number) of surface in each category of intensity.

In order to calibrate the digital analysis algorithm, a preliminary comparison of semiquantitative visual assessment and quantitative analysis using image

Table 1 Demographic and clinicopathological characteristics of the patients

Characteristics	*Patients (*n = *170)*
Age (years), mean s.d.	60.2 (11.7)
Age groups (years), n *(%)*	
<50	36 (21)
50–59	48 (28)
60–69	46 (27)
≥70	40 (24)
FIGO stage, n *(%)*	
I	32 (19)
II	15 (9)
IIIa–b	4 (2)
IIIc	101 (59)
IV	18 (11)
Histology, n *(%)*	
Serous	118 (69)
Clear cell	23 (14)
Endometrioid	17 (10)
Others	12 (7)
Grade, n *(%)*	
Low (Silverberg grade 1)	28 (17)
High (Silverberg grades 2–3)	142 (84)
CA-125 preoperative level (U/ml), median (IQR)[a]	465 (170.5–1180.0)
Progression status at last follow-up	
No	53 (31)
Yes	117 (69)
Death	
Alive	66 (39)
Dead	104 (61)

[a]IQR, interquartile range (interval between the 25th and the 75th percentile).

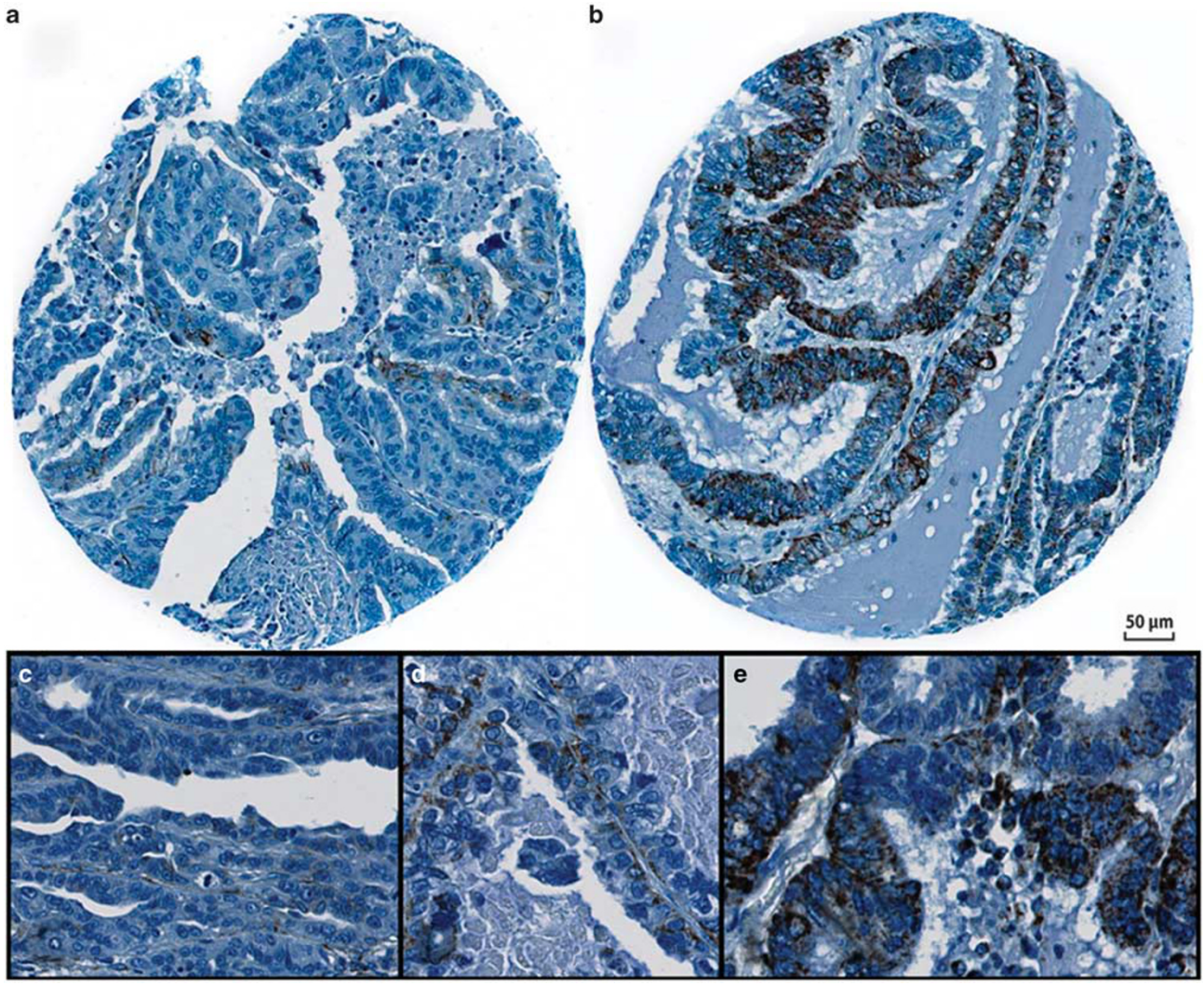

Figure 2 Matrix metalloproteinase-14 expression was found in 66% of the cases. Representative ovarian carcinoma tissue microarray spots with (**a**) low and (**b**) high proportion of immunostaining showed. Representative samples of (**c**) low (1), (**d**) moderate (2) and (**e**) high (3) immunostaining intensity as visually scored.

analysis was performed on a training set consisting of 58 tissue microarray spots of women not eligible for the main statistical analyses. Those spots covered all visual percentage classes. A strong association was observed between visual assessment and digital image analysis (Spearman's correlation coefficient $\rho = 0.84$; $P < 0.0001$).

All digital assessments were performed on tissue microarray spots on $10\times$ resolution images and results were revised visually. When the tissue recognition provided by the segmentation algorithm was judged unsatisfactory, a gross manual segmentation was done before relaunching the Ilastik algorithm and performing the immunosurface analysis.

Statistical Analysis

The statistical analyses were conducted using SAS 9.2 (SAS Institute, Cary, NC, USA). All tests were two sided. Analyses were done according to the Guidelines for the REporting of tumor MARKer Studies (REMARK).[24]

As few cases showed >40% of positive cells by visual analysis, tumors having >40% of positive cells were grouped, leading to the following classes: 0%, 1–20%, 21–40%, and 41–100%. For similar reasons, categories of intensity were dichotomized (2–3 *vs* 0–1). For each tumor, the mean of the percentage of staining was calculated and the highest intensity score was measured. For digital image analysis results, the mean number of cells of the highest intensity (category 3), the mean global percent of immunostaining, as well as the average H-score[25] were used. The two latter measures were further classified by quartiles that were used to describe MMP-14 immunostaining according to ovarian cancer standard prognostic factors. The highest levels of MMP-14 expression were defined as: (1) >40% of MMP-14-positive cells when assessed visually and (2)

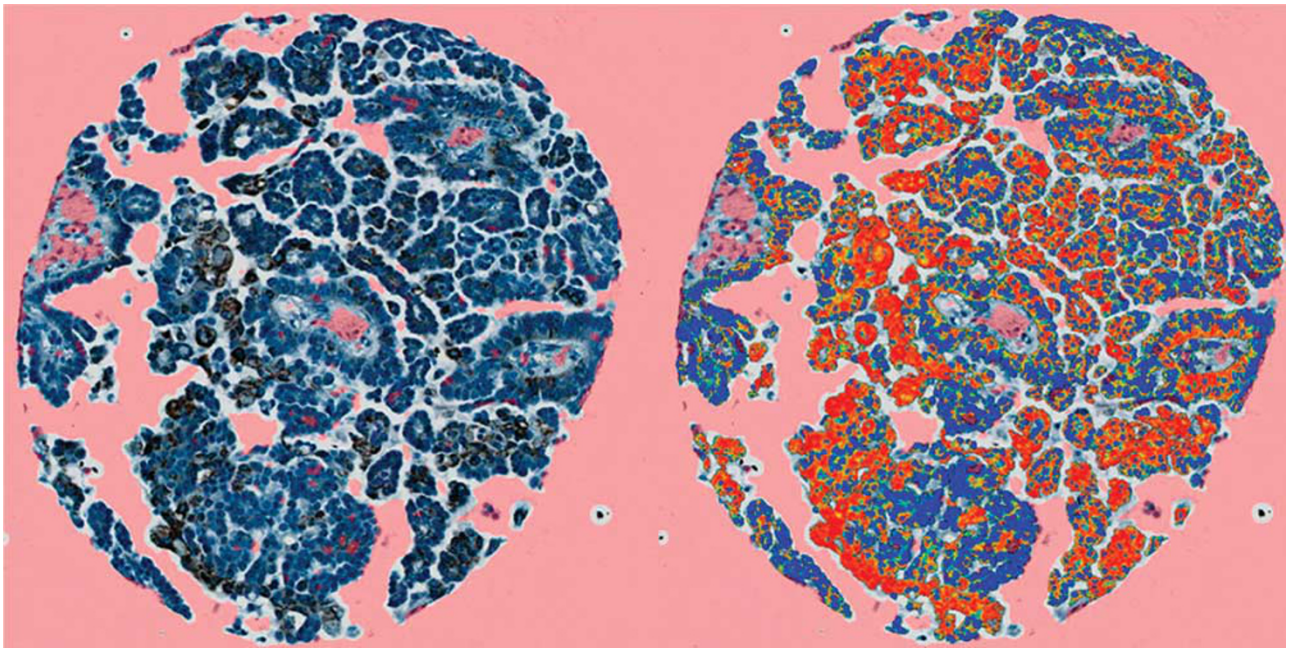

Figure 3 Matrix metalloproteinase-14 immunostaining. Tissue microarray spot sample showing segmentation mask application (left) and corresponding immunosurface algorithm result (right; blue = negative, yellow = low intensity, orange = moderate intensity and red = high intensity).

Table 2 Distribution of women with ovarian carcinoma according to the percentage of matrix metalloproteinase-14 (MMP-14)-positive cells (visual) and positive area (digital image analysis) and standard prognostic factors

	% MMP-14-positive cells, visual scoring (total n = *160)*					*% MMP-14-positive area, digital image analysis, per quartile (total* n = *170)*				
	0 n/*55 (%)*	*1–20* n/*45 (%)*	*21–40* n/*42 (%)*	*>40* n/*18 (%)*	P	*1st* n/*43 (%)*	*2nd* n/*42 (%)*	*3rd* n/*43 (%)*	*4th* n/*42 (%)*	P
Age group (years)										
<50	7 (13)	14 (31)	10 (24)	5 (28)	0.3	10 (23)	8 (19)	6 (14)	12 (29)	0.2
50–59	19 (35)	10 (22)	12 (29)	4 (22)		13 (30)	9 (21)	15 (35)	11 (26)	
60–69	16 (29)	8 (18)	14 (33)	6 (33)		7 (16)	13 (31)	11 (26)	15 (36)	
≥70	13 (24)	13 (29)	16 (14)	3 (17)		13 (30)	12 (29)	11 (26)	4 (10)	
FIGO stage										
I–II	9 (16)	9 (20)	17 (41)	12 (67)	<0.0001	8 (19)	7 (17)	12 (28)	20 (48)	0.005
III–IV	46 (84)	36 (80)	25 (60)	6 (33)		35 (81)	35 (83)	31 (72)	22 (52)	
Histology										
Serous	46 (84)	37 (82)	20 (48)	5 (28)	<0.0001	36 (84)	36 (86)	29 (67)	17 (41)	<0.0001
Others	9 (16)	8 (18)	22 (52)	13 (72)		7 (16)	6 (14)	14 (33)	25 (60)	
Grade										
Low	8 (15)	6 (13)	7 (17)	4 (22)	0.8	7 (16)	6 (14)	6 (14)	9 (21)	0.8
High	47 (86)	39 (87)	35 (83)	14 (78)		36 (84)	36 (86)	37 (86)	33 (79)	
Preoperative CA-125, quartiles (U/ml)										
0–151	6 (11)	10 (22)	11 (26)	8 (44)	0.02	8 (19)	6 (14)	5 (12)	17 (41)	0.02
152–441	17 (31)	9 (20)	10 (24)	4 (22)		10 (23)	13 (31)	12 (28)	8 (19)	
442–1179	17 (31)	12 (27)	4 (10)	5 (28)		12 (28)	15 (36)	10 (23)	5 (12)	
≥1180	15 (27)	14 (31)	17 (41)	1 (6)		13 (30)	8 (19)	16 (37)	12 (29)	

the higher quartile of MMP-14-positive area when assessed by digital image analysis. The χ^2 tests were performed to assess the difference of MMP-14 expression according to standard prognostic factors.

Progression-free survival was calculated from the date of cytoreductive surgery to the date of progression, death, or most recent follow-up visit. Overall survival (OS) was calculated from the date of

Table 3 Distribution of women with ovarian carcinoma according to matrix metalloproteinase-14 (MMP-14) immunostaining (mean cell number of the highest intensity (digital image analysis), average H-score (digital image analysis), intensity (visual)), and standard prognostic factors ($n=170$)

	Mean cell number of the highest intensity			*Average H-score*			*Maximal intensity (visual)*		
	Q1–Q3 n/*128 (%)*	*Q4* n/*42 (%)*	P	*Q1–Q3* n/*127 (%)*	*Q4* n/*43 (%)*	P	*0 or 1* n/*98 (%)*	*2 or 3* n/*62 (%)*	P
Age group (years)									
<50	26 (20)	10 (24)	0.7	24 (19)	12 (28)	0.17	18 (18)	18 (29)	0.2
50–59	35 (27)	13 (31)		35 (28)	13 (30)		29 (30)	16 (26)	
60–69	34 (27)	12 (29)		33 (26)	13 (30)		25 (26)	19 (31)	
≥70	33 (26)	7 (17)		35 (27)	5 (12)		26 (27)	9 (15)	
FIGO stage									
I–II	28 (22)	19 (45)	0.003	28 (22)	19 (44)	0.005	16 (16)	31 (50)	<0.0001
III–IV	100 (78)	23 (55)		99 (78)	24 (56)		82 (84)	31 (50)	
Histology									
Serous	97 (76)	21 (50)	0.001	101 (80)	17 (40)	<0.0001	78 (80)	30 (48)	<0.0001
Others	31 (24)	21 (50)		26 (21)	26 (61)		20 (20)	32 (52)	
Grade									
Low	18 (14)	10 (24)	0.1	19 (15)	9 (21)	0.36	15 (15)	10 (16)	0.9
High	110 (86)	32 (76)		108 (85)	34 (79)		83 (85)	52 (84)	
Preoperative CA-125, quartiles (U/ml)									
0–151	22 (17)	14 (33)	0.01	20 (16)	16 (37)	0.003	14 (14)	21 (34)	0.03
152–441	36 (28)	7 (17)		35 (28)	8 (19)		28 (29)	12 (19)	
442–1179	37 (29)	5 (12)		38 (30)	4 (9)		26 (27)	12 (19)	
≥1180	33 (26)	16 (38)		34 (27)	15 (35)		30 (31)	17 (27)	

cytoreductive surgery to the date of death or last contact. Kaplan–Meier curves and log-rank tests were performed to assess the effect of the percent of MMP-14-positive area assessed by digital image analysis on progression and death. Multivariate Cox proportional hazard regression models were built to assess the relationships between MMP-14 immunostaining variables and prognosis. Crude and adjusted hazard ratios were estimated, with their 95% confidence intervals. For each outcome, all standard prognostic factors—age (continuous), FIGO stage (I–II *vs* III–IV), histology (serous *vs* others), grade (1 *vs* 2–3), and preoperative CA-125 levels (<465 U/ml *vs* ≥465 U/ml (median value))—were included in the multivariate models. The residual disease variable was not included in the multivariate models, as a strong association between the residual tumor and the FIGO stage was observed ($P<0.0001$). Subgroup analyses were conducted among women with serous carcinoma using the Cox multivariate model taking into account the grade (low *vs* high), the FIGO stage (I–II *vs* III–IV), the age (continuous), and the preoperative CA-125 (>442 or ≤442 U/ml (median)).

Box plots were constructed to describe the distribution of the percentage of MMP-14-positive area (continuous variable) assessed by digital image analysis according to the same measure assessed visually (categorical variable). The Kruskal–Wallis test, followed by the Dunn test when appropriate, was used to verify the differences between the distributions of digital image analysis positive area scores according to the visual assessment classes.

Results

Population and Clinicopathological Characteristics

Out of 243 women with a primary diagnostic of ovarian carcinoma, 32 were excluded because they had neoadjuvant chemotherapy, nononcologic surgery, or no adjuvant chemotherapy (Figure 1). Among the 211 eligible women, MMP-14 immunostaining could be evaluated in 160 (visual assessment) and in 170 (digital assessment) tumors. The difference in the number of evaluated cases by both methods was related to discrepancies in the evaluation of the 30% of tumor surface threshold used to determine interpretability. Of the 170 women who could be evaluated by digital image analysis, 101 (59%) had FIGO stage III disease and 118 (69%) had a serous histology. Most other tumors were either clear cell ($n=23$, 14%) or endometrioid ($n=17$, 10%). The median follow-up until progression was 1.6 years and the median follow-up until death was 5.2 years. During this time, 117 women experienced disease progression and 104 died of disease.

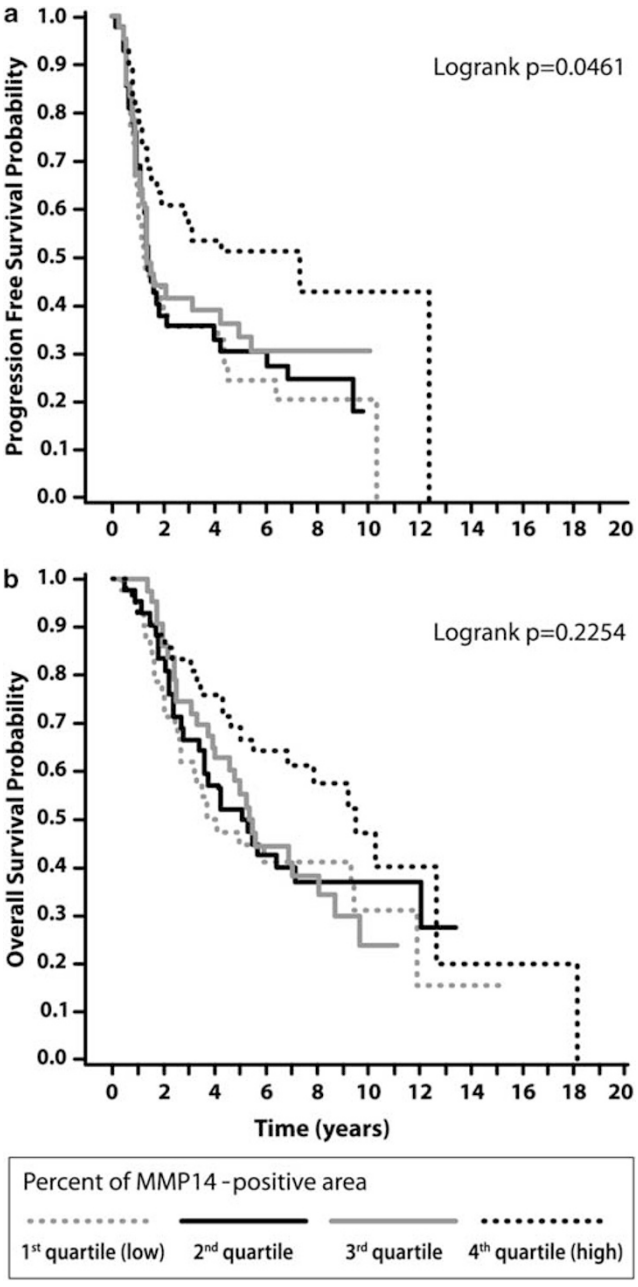

Figure 4 (**a**) Progression-free survival and (**b**) overall survival of ovarian cancer in women according to the quartile of percent of matrix metalloproteinase-14 (MMP-14)-positive area obtained with digitalized image analysis (1st quartile: 0.7 to 2.6; 2nd quartile: 2.6 to 5.6; 3th quartile: 5.6 to 11.2; 4th quartile: 11.2 to 80.6).

The detailed patient demographic and clinicopathological characteristics are shown in Table 1.

Immunohistochemistry

MMP-14 was expressed in 105 cases (66%) (Figure 2). The immunostaining was cytoplasmic and nongranular. High intensity (maximal intensity score ≥ 2) was found in 62 cases (39%). The median percent of MMP-14-positive area estimated by digital image analysis was 5.56 (interquartile range: 2.62–11.16). An example of the masks generated during the virtual analysis is shown in Figure 3.

Associations between MMP-14 Immunostaining, Standard Prognostic Factors, OS, and Progression-Free Survival

The highest levels of MMP-14 expression were associated with early stage (FIGO I–II), nonserous histology, and low preoperative CA-125 when assessed visually and by digital image analysis (Table 2). Similar associations were observed between standard prognostic factors and MMP-14 intensity, the highest intensity mean cell number, and the average H-score[25] (Table 3).

Using Kaplan–Meier curves, we showed that the percentage of MMP-14-positive area as assessed by digital image analysis was significantly associated with progression ($P=0.046$), but not with death ($P=0.23$) (Figure 4). The highest level of MMP-14-positive cells as visually assessed was associated with a lower risk of progression (hazard ratio: 0.39, 95% confidence interval: 0.18–0.82, $P=0.01$). A similar inverse association between the highest level of MMP-14-positive area and the risk of progression was observed when the assessments were done by digital image analysis (hazard ratio: 0.48, 95% confidence interval: 0.28–0.82, $P=0.008$; Table 4). There was an association of borderline significance between the highest level of MMP-14-positive area assessed by digital image analysis and death (hazard ratio: 0.57, 95% confidence interval: 0.32–1.00, $P=0.05$). Although the hazard ratio was similar (0.52) when MMP-14 expression was assessed visually, this association was not significant ($P=0.10$). Similar results were obtained using the other measurements of MMP-14 immunostaining (Table 5). In multivariate analyses, MMP-14 expression was not associated with either progression or death, regardless of the assessment method (Table 4).

In women with serous carcinoma, the multivariate analyses showed that the highest level of MMP-14-positive area assessed by digital image analysis was significantly associated with a lower risk of progression (adjusted hazard ratio: 0.48, 95% confidence interval: 0.24–0.99, $P=0.046$), but not with death (adjusted hazard ratio: 0.70, 95% confidence interval: 0.35–1.43).

Association between Visual and Digital Analysis

Box plots were used to describe the digital image analysis measures according to the visual assessment (Figure 5). The percent of MMP-14-positive area assessed with the digital image analysis was underestimated compared with the percentage of positive cells assessed visually. All comparisons of percent

Table 4 Adjusted hazard ratios of death and progression of ovarian carcinoma and their 95% confidence intervals associated with the percentage of matrix metalloproteinase-14 (MMP-14)-positive cells (visual) and positive area (digital image analysis)

	Death				*Progression*			
	Crude hazard ratios (95% confidence interval)	P	*Adjusted hazard ratios[a] (95% confidence interval)*	P	*Crude hazard ratios (95% confidence interval)*	P	*Adjusted hazard ratios[a] (95% confidence interval)*	P
Percent of MMP-14-positive cells, visual scoring (n = *160)*								
>40	0.52 (0.24–1.13)	0.10	1.08 (0.47–2.49)	0.86	0.39 (0.18–0.82)	0.01	0.88 (0.39–2.00)	0.76
21–40	0.91 (0.55–1.52)	0.72	1.17 (0.66–2.07)	0.59	0.67 (0.41–1.09)	0.10	1.00 (0.59–1.69)	0.98
1–20	0.93 (0.56–1.54)	0.78	1.07 (0.64–1.79)	0.79	0.80 (0.50–1.27)	0.34	0.94 (0.58–1.52)	0.80
0	1	—	1	—	1	—	1	—
Percent of MMP-14-positive area, digital image analysis, per quartile (n = *170)*								
4th	0.57 (0.32–1.00)	0.05	0.83 (0.46–1.52)	0.55	0.48 (0.28–0.82)	0.008	0.73 (0.41–1.29)	0.28
3rd	0.90 (0.53–1.54)	0.71	0.91 (0.53–1.58)	0.75	0.77 (0.47–1.26)	0.30	0.85 (0.51–1.41)	0.52
2nd	0.88 (0.51–1.50)	0.63	0.8 (0.47–1.39)	0.45	0.89 (0.55–1.45)	0.64	0.83 (0.51–1.36)	0.46
1st	1	—	1	—	1	—	1	—

[a]Model was adjusted for grade (low *vs* high), stage (I–II *vs* III–IV), histology (serous *vs* others), age (continuous), and preoperative CA-125 (>442 or ≤442 U/ml (median)).

Table 5 Adjusted hazard ratios of death and progression of ovarian carcinoma and their 95% confidence intervals associated with quantitative matrix metalloproteinase-14 immunostaining

	Death				*Progression*			
	Crude hazard ratios (95% confidence interval)	P	*Adjusted hazard ratios[a] (95% confidence interval)*	P	*Crude hazard ratios (95% confidence interval)*	P	*Adjusted hazard ratios[a] (95% confidence interval)*	P
Mean cell number of the highest intensity, quartile 4 vs *quartiles 1–3* (n = *170)*								
Q4	0.63 (0.39–1.02)	0.06	0.82 (0.50–1.33)	0.42	0.60 (0.37–0.95)	0.03	0.75 (0.47–1.21)	0.24
Q1–Q3	1	—	1	—	1	—	1	—
Average H-score, quartile 4 vs *quartiles 1–3* (n = *170)*								
Q4	0.60 (0.37–0.96)	0.04	0.80 (0.48–1.33)	0.38	0.54 (0.34–0.87)	0.01	0.72 (0.44–1.18)	0.19
Q1–Q3	1	—	1	—	1	—	1	—
Maximal intensity (visual) (n = *160)*								
2 or 3	0.61 (0.40–0.94)	0.02	0.87 (0.55–1.37)	0.54	0.49 (0.33–0.75)	0.001	0.75 (0.48–1.17)	0.2
0 or 1	1	—	1	—	1	—	1	—

[a]Model was adjusted for grade (low *vs* high), stage (I–II *vs* III–IV), histology (serous *vs* others), age (continuous), and preoperative CA-125 (>442 or ≤442 U/ml (median)).

of MMP-14-positive area assessed by digital image analysis between the four classes of visual assessment were statistically significant except for the two first categories (0% and 1–20%), suggesting to group them. This showed that the digital image analysis assessment matched the visual assessment in three categories: 0–20%, 21–40%, and >40%.

Discussion

This study was aimed at investigating whether the expression of MMP-14 as detected by immunohistochemistry could be used as a prognostic biomarker in ovarian cancer, as assessed both visually on digital slides and by digital image analysis. We showed that the highest levels of MMP-14 expression were associated with early-stage disease (FIGO I–II), nonserous histology, and low preoperative CA-125. In the cohort of women with ovarian carcinoma, the highest level of MMP-14-positive area was associated with a lower risk of progression in the bivariate analyses, although it had no effect on either progression or death after taking into account standard prognostic factors of ovarian carcinoma. In women with serous carcinoma, the highest level of MMP-14-positive area was significantly associated with a lower risk of progression after taking into account standard prognostic factors of ovarian carcinoma.

MMP-14 expression in ovarian cancer has been demonstrated,[13,14] but few studies have addressed

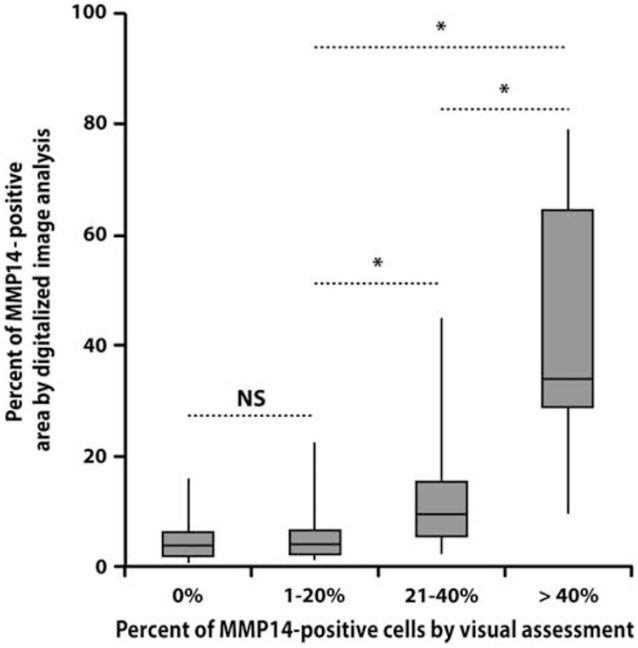

Figure 5 Box plot distribution of matrix metalloproteinase-14 (MMP-14)-positive area assessment obtained by digitalized image analysis according to visual assessment categories performed by pathologists. $^*P<0.05$; NS, no significant difference.

the prognostic impact of MMP-14 as evaluated by immunohistochemistry.[16,26] Kamat *et al*[16] showed that high MMP-14 expression was associated with both aggressive ovarian cancer characteristics and poor prognostic, whereas Brun *et al*[26] did not report any associations between MMP-14 and prognosis. We here report different results that can be partly explained by different methods of MMP-14 assessment and by the selection of a different cohort of women with ovarian carcinoma. Similar to Kamat *et al*,[16] we used a rabbit polyclonal antibody, but we detected only 65% of positive cases as compared with 100% in their study. This could be explained by the difference in our antigen revelation strategies that could lead to different expression patterns.[27] The population studied by Brun *et al*[26] included 38% of women treated by neoadjuvant chemotherapy, in which they report higher expression of MMP-14. One limitation of this study is the relatively small size of the cohort ($n=69$) that could have prevented them from detecting a significant association between MMP-14 expression and progression-free survival.

In women with serous carcinoma, the highest quartile of MMP-14-positive area, as assessed by digital image analysis, was significantly associated with a lower risk of progression after taking into account standard prognostic factors of ovarian carcinoma. This result is compatible with the emerging hypothesis in which high-grade serous ovarian carcinoma is a distinct type of disease[28,29] that constituted 85% of our subgroup of women with serous ovarian cancer. We believe that more information could be gained about the effect of MMP-14 expression in ovarian carcinoma if further studies included a subgroup analysis for women with serous ovarian cancer. Very large cohorts of women with ovarian carcinoma could be used to refine our understanding of the effect of MMP-14 expression in ovarian carcinoma by including stratified analyses for women with type I and II carcinoma, the latter including high-grade serous carcinoma, malignant mixed Müllerian tumor, and undifferentiated carcinoma.[28,29]

MMP-14 leads to the activation of MMP-2 by binding to TIMP-2 and forming a complex with pro-MMP-2.[30,31] As expected, mRNA studies showed a close relationship between MMP-14 and MMP-2 in ovarian carcinoma and pleural effusions, with some being related to poor outcome.[14,15,17,32] Torng *et al*[33] also observed the colocalization of MMP-2 and MMP-14 as detected by immunohistochemistry in ovarian carcinoma. In our study, MMP-14 was associated with early stage and low preoperative CA-125 levels. This could be consistent with an early expression of MMP-14 in the ovarian cancer environment, potentially leading to the activation of MMP-2.

This study also provided an assessment of digital image analysis technology efficacy in morphologically complex tissues such as ovarian carcinoma. Using commercially available software algorithms to classify the epithelial component of tumors and quantify immunostaining, we could reproduce immunohistochemistry data obtained by visual assessment done by pathologists in terms of percent of positive cells and relationship with clinicopathological factors. Both types of analyses also identified the asymmetric distribution of MMP-14 as few tumors were found among those with the highest levels of expression. When assessed by digital image analysis, 75% of women had tumors expressing MMP-14 in 0 to 11% of the whole tumor area, whereas the remaining 25% had tumors expressing MMP-14 in 11 to 81%. We noted a tendency of digital image analysis to underestimate the positive surface of staining that is due in part to the algorithm chosen. The digital image analysis algorithm measures the percent of positive staining in the whole cell surface, including the negative nuclei surface. This produces a value systematically lower than the visual analysis, as pathologists can evaluate the cytoplasm without including the nuclei in the assessment. However, the associations with prognosis remained consistent with both methods of assessment.

There are many reports of data provided by software algorithms that correlate well with pathologist semiquantitative scores, for example in breast cancer for HER2 and receptor status.[34–36] Rizzardi *et al*[37] also reported a good performance of computer-assisted image classification and immunohistochemistry quantification in ovarian serous carci-

noma. Our algorithms performed well in the highly varied histologic types of ovarian carcinoma, with a relatively low level of manual correction needed (~8%, data not shown). Thus, our results suggest that digital image analysis can be used in quantitative immunohistochemistry evaluation of cytoplasmic markers in ovarian carcinoma, with the advantage of providing reproducible quantitative measures. In the context of tissue microarray biomarker studies, digital image analysis offers an interest in time conservation for pathologists and a protection from the effect of fatigue on data quality.

Our results showed that MMP-14 expression is associated with better standard factors of ovarian carcinoma prognosis, but that MMP-14 is not an independent prognostic factor for women with ovarian carcinoma. However, in women with serous carcinoma, high levels of MMP-14 expression were significantly associated with lower progression. We also showed that digital image analysis can be used for quantitative measurements of immunohistochemistry staining, even for a cytoplasmic marker.

Acknowledgments

This research has been funded by the Cancer Research Society and was conducted with tissues obtained from the *Banque de tissus et de données* of the *Réseau de recherche sur le cancer* of the *Fonds de la recherche du Québec*-Santé (FRQS), affiliated to the Canadian Tumor Repository Network (CTRNet). DT was a recipient of a doctoral research award from the Fonds de la Recherche en Santé du Québec (FRSQ), and is now part of The Terry Fox Foundation Strategic Health Research Training Program in Cancer Research at the Canadian Institute of Health Research (CIHR) and the Ontario Institute of Cancer Research (OICR). Thanks to Éric Morin for his help with figure editing.

Disclosure/conflict of interest

The authors declare no conflict of interest.

References

1 Holschneider CH, Berek JS. Ovarian cancer: epidemiology, biology, and prognostic factors. Semin Surg Oncol 2000;19:3–10.
2 Jemal A, Siegel R, Ward E, *et al.* Cancer statistics 2008) CA Cancer J Clin 2008;58:71–96.
3 Canadian Cancer Society's steering Committee on Cancer Statistics. Canadian Cancer Statistics 2011. Canadian Cancer Society: Toronto, ON, 2011. Report No. 0835-2976.
4 Guarneri V, Piacentini F, Barbieri E, Conte PF. Achievements and unmet needs in the management of advanced ovarian cancer. Gynecol Oncol 2010;117:152–158.
5 Cannistra SA. Cancer of the ovary. N Engl J Med 2004;351:2519–2529.
6 Petit T, Velten M, d'Hombres A, *et al.* Long-term survival of 106 stage III ovarian cancer patients with minimal residual disease after second-look laparotomy and consolidation radiotherapy. Gynecol Oncol 2007;104:104–108.
7 Overall CM, Kleifeld O. Tumour microenvironment - opinion: validating matrix metalloproteinases as drug targets and anti-targets for cancer therapy. Nat Rev Cancer 2006;6:227–239.
8 Kessenbrock K, Plaks V, Werb Z. Matrix metalloproteinases: regulators of the tumor microenvironment. Cell 2010;141:52–67.
9 Moss NM, Barbolina MV, Liu Y, *et al.* Ovarian cancer cell detachment and multicellular aggregate formation are regulated by membrane type 1 matrix metalloproteinase: a potential role in I.p. metastatic dissemination. Cancer Res 2009;69:7121–7129.
10 Bourboulia D, Stetler-Stevenson WG. Matrix metalloproteinases (MMPs) and tissue inhibitors of metalloproteinases (TIMPs): positive and negative regulators in tumor cell adhesion. Semin Cancer Biol 2010;20: 161–168.
11 Itoh Y, Seiki M. MT1-MMP: a potent modifier of pericellular microenvironment. J Cell Physiol 2006; 206:1–8.
12 Barbolina MV, Adley BP, Ariztia EV, Liu Y, Stack MS. Microenvironmental regulation of membrane type 1 matrix metalloproteinase activity in ovarian carcinoma cells via collagen-induced EGR1 expression. J Biol Chem 2007;282:4924–4931.
13 Fishman DA, Bafetti LM, Stack MS. Membrane-type matrix metalloproteinase expression and matrix metalloproteinase-2 activation in primary human ovarian epithelial carcinoma cells. Invasion Metastasis 1996;16:150–159.
14 Afzal S, Lalani EN, Poulsom R, *et al.* MT1-MMP and MMP-2 mRNA expression in human ovarian tumors: possible implications for the role of desmoplastic fibroblasts. Hum Pathol 1998;29:155–165.
15 Sakata K, Shigemasa K, Nagai N, Ohama K. Expression of matrix metalloproteinases (MMP-2, MMP-9, MT1-MMP) and their inhibitors (TIMP-1, TIMP-2) in common epithelial tumors of the ovary. Int J Oncol 2000;17:673–681.
16 Kamat AA, Fletcher M, Gruman LM, *et al.* The clinical relevance of stromal matrix metalloproteinase expression in ovarian cancer. Clin Cancer Res 2006;12:1707–1714.
17 Davidson B, Goldberg I, Gotlieb WH, *et al.* The prognostic value of metalloproteinases and angiogenic factors in ovarian carcinoma. Mol Cell Endocrinol 2002;187:39–45.
18 Riber-Hansen R, Vainer B, Steiniche T. Digital image analysis: a review of reproducibility, stability and basic requirements for optimal results. APMIS 2012;120: 276–289.
19 Walker RA. Quantification of immunohistochemistry–issues concerning methods, utility and semiquantitative assessment I. Histopathology 2006;49:406–410.
20 Stuart GC, Kitchener H, Bacon M, *et al.* 2010 Gynecologic Cancer InterGroup (GCIG) consensus statement on clinical trials in ovarian cancer: report from the Fourth Ovarian Cancer Consensus Conference. Int J Gynecol Cancer 2011;21:750–755.
21 Eisenhauer EA, Therasse P, Bogaerts J, *et al.* New response evaluation criteria in solid tumours: revised RECIST guideline (version 1.1). Eur J Cancer 2009;45: 228–247.

22 Sundar S, O'Byrne KJ. CA-125 criteria for response evaluation in ovarian cancer. Gynecol Oncol 2005;98:520–521.
23 Silverberg SG. Histopathologic grading of ovarian carcinoma: a review and proposal. Int J Gynecol Pathol 2000;19:7–15.
24 McShane LM, Altman DG, Sauerbrei W, *et al.* Reporting recommendations for tumor marker prognostic studies. J Clin Oncol 2005;23:9067–9072.
25 Clark BZ, Dabbs DJ, Cooper KL, Bhargava R. Impact of progesterone receptor semiquantitative immunohistochemical result on Oncotype DX recurrence score: a quality assurance study of 1074 cases. Appl Immunohistochem Mol Morphol 2013;21:287–291.
26 Brun JL, Cortez A, Lesieur B, *et al.* Expression of MMP-2, -7, -9, MT1-MMP and TIMP-1 and -2 has no prognostic relevance in patients with advanced epithelial ovarian cancer. Oncol Rep 2012;27: 1049–1057.
27 Leong TY, Leong AS. How does antigen retrieval work? Adv Anat Pathol 2007;14:129–131.
28 McCluggage WG. Morphological subtypes of ovarian carcinoma: a review with emphasis on new developments and pathogenesis. Pathology 2011;43:420–432.
29 Bast RC Jr, Hennessy B, Mills GB. The biology of ovarian cancer: new opportunities for translation. Nat Rev Cancer 2009;9:415–428.
30 Strongin AY, Collier I, Bannikov G, *et al.* Mechanism of cell surface activation of 72-kDa type IV collagenase. Isolation of the activated form of the membrane metalloprotease. J Biol Chem 1995;270:5331–5338.
31 Strongin AY. Proteolytic and non-proteolytic roles of membrane type-1 matrix metalloproteinase in malignancy. Biochim Biophys Acta 2010;1803:133–141.
32 Davidson B, Reich R, Berner A, *et al.* Ovarian carcinoma cells in serous effusions show altered MMP-2 and TIMP-2 mRNA levels. Eur J Cancer 2001;37:2040–2049.
33 Torng PL, Mao TL, Chan WY, Huang SC, Lin CT. Prognostic significance of stromal metalloproteinase-2 in ovarian adenocarcinoma and its relation to carcinoma progression. Gynecol Oncol 2004;92:559–567.
34 Brugmann A, Eld M, Lelkaitis G, *et al.* Digital image analysis of membrane connectivity is a robust measure of HER2 immunostains. Breast Cancer Res Treat 2012;132:41–49.
35 Joshi AS, Sharangpani GM, Porter K, *et al.* Semiautomated imaging system to quantitate Her-2/neu membrane receptor immunoreactivity in human breast cancer. Cytometry A 2007;71:273–285.
36 Sharangpani GM, Joshi AS, Porter K, *et al.* Semiautomated imaging system to quantitate estrogen and progesterone receptor immunoreactivity in human breast cancer. J Microsc 2007;226:244–255.
37 Rizzardi AE, Johnson AT, Vogel RI, *et al.* Quantitative comparison of immunohistochemical staining measured by digital image analysis versus pathologist visual scoring. Diagn Pathol 2012;7:42.